International Journal Of
Industrial Electronics Control and Optimization
Print ISSN: 3517-2645
Online ISSN: 3568-2645
Homepage: https://ieco.usb.ac.ir/

Enhancing Small-Signal Stability of Multi-Machine Power Systems Using PMU Data

Zivar Rigi | Mahdi Hassanniakheibari

Department of Electrical Engineering, ZAH.C., Islamic Azad University, Zahedan, Iran.[1,2]
Corresponding author's email: mahdi.hassannia@iau.ac.ir

Article Info

Article type:
Research Article

Article history:
Received: 07-August-2025
Received in revised form:
26—October-2025
Accepted: 06-November-2025
Published online: 21-March-2026

Keywords:
PMU data,
PSD and CSD methods,
Small signal,
Stability analysis,
14-bus IEEE system.

ABSTRACT

As power systems rapidly expand and the demand for uninterrupted power supply to network loads increases, ensuring the safe and stable operation of these systems has become crucially important. However, conducting dynamic stability assessments with detailed dynamic models is nearly impossible in today's complex power networks. The introduction of Phasor Measurement Units (PMUs) has paved the way for new stability evaluation techniques that rely on real-time measurement data. A common limitation of most measurement-based techniques is their vulnerability to noise in the data. While some newer methods offer improved noise resistance, they are often hindered by high computational demands and slow processing times, limiting their practical use. This paper developed a measurement-based method that uses power spectral density (PSD) and cross-spectral density (CSD) to achieve a more precise estimation of low-frequency oscillations in power systems. Simulation results on the IEEE 14-bus and 39-bus test systems, tested under both noisy and noise-free conditions, show that the proposed method yields more accurate frequency and oscillation shape estimates, even when measurement noise is present. Additionally, the Prony algorithm, a well-known measurement-based method, is also implemented, and its high sensitivity to noisy data is demonstrated.

NOMENCLATURE

H	Inertia constant of the generator-turbine system	K_S	Synchronizing coefficient
ω	Rotor speed	K_D	Damping coefficient
ω_o	Synchronous electrical speed	A	State matrix
$\Delta\omega_r$	Rotor speed deviation (per unit)	B	Input matrix
δ	Rotor angle	$x(t)$	State vector
$\Delta\delta$	Rotor angle deviation	$u(t)$	Input vector
P_{mech}	Mechanical power input	$z_i(t)$	Modal state of the i-th mode
P_e	Electrical power output	λ_i	Eigenvalue of the i-th mode
T_D	Damping torque	R_i, L_i	Right and left eigenvectors corresponding to λ_i
P_D	Damping power	$S_{kk}(\omega)$	Power Spectral Density (PSD) of signal y_k
X_T	Total reactance (machine + line)	$S_{kl}(\omega)$	Cross Spectral Density (CSD) between signals y_k and y_l
X_D'	Transient reactance of the generator	$Y_k(\omega)$	Fourier transform of signal $y_k(t)$
X_E	Line reactance	$Z_i(\omega)$	Frequency domain representation of modal response
$\acute{E}$	Internal transient voltage	$S_x^{\omega}(\omega_k)$	Welch's averaged periodogram estimate
E_B	Infinite bus voltage		

I. Introduction

Recent operational experience with multi-machine power systems has revealed that power oscillations, especially during heavy loading of transmission lines, are common occurrences. When these oscillations persist or intensify, they pose a significant risk to the overall stability of the system [1–8]. Under such conditions, the rotors of synchronous generators begin to oscillate, which in the worst case can lead to a total loss of synchronism within the whole

network [9]. The large-scale blackout in the Western Electricity Coordinating Council (WECC) region in 1996 highlighted to operators and power system engineers the vital need for effective monitoring and control of low-frequency oscillations [10].

Consequently, precise and real-time detection of low-frequency oscillations within today's complex multi-machine power networks is crucial for preserving system synchronism and averting large-scale blackouts. Current research on identifying these oscillatory modes generally falls into two primary approaches:

- Model-based analytical methods that utilize dynamic system representations,
- Measurement-based techniques grounded in signal processing.

Traditional model-based approaches, such as modal analysis, require linearizing the system around a stable operating point, and the identification of oscillatory modes depends heavily on having detailed knowledge of the system's dynamic model [11]. However, obtaining accurate models of large-scale, interconnected power networks is highly challenging and frequently unreliable. Moreover, even assuming full model availability, developing a real-time control system capable of rapidly and precisely responding to system oscillations remains practically unfeasible.

Conversely, the advent of Phasor Measurement Units (PMUs) and the implementation of Wide Area Measurement Systems (WAMS) have facilitated the provision of high-resolution, time-synchronized data to control centers [12]. This technological progress has enabled the application of a variety of signal processing techniques for oscillation analysis, such as Fast Fourier Transform (FFT) [13], wavelet transform [14], Prony analysis [15], Stochastic Subspace Identification (SSI) [16], Auto-Regressive Moving Average (ARMA) modeling [17], and Hilbert-Huang Transform (HHT) [18]. While these methods facilitate faster detection of oscillatory phenomena, they also present inherent limitations. For instance, the Fast Fourier Transform (FFT) estimates only the dominant frequency and cannot track instantaneous damping, rendering it ineffective for analyzing nonlinear or non-stationary signals. The Wavelet Transform utilizes localized wavelets with finite duration and zero mean [19]. Despite its strength in capturing time-frequency characteristics, it encounters challenges such as frequency overlap and difficulties in selecting appropriate wavelet bases.

Prony analysis, as a well-known measurement-based method, can rapidly extract dominant oscillatory modes but is highly sensitive to noise and becomes unreliable when multiple signal components coexist [20]. Comparative studies with FFT and eigenvalue analysis [21], [22] have demonstrated Prony's superiority in extracting oscillatory features. A modified Prony technique incorporating signal subspace theory was proposed in [23] to mitigate noise sensitivity; however, it still exhibits some vulnerability to noise. Another approach based on noise subspace decomposition, introduced in [24], identifies low-frequency modes by applying a median filter to reduce variability in mode estimation. Comparative analyses indicate this method surpasses conventional Prony analysis in terms of frequency standard deviation and damping accuracy [25], [26].

Several investigations [27–30] have employed subspace estimation methods, such as Principal Component Analysis (PCA) and Stochastic Subspace Identification (SSI), for low-frequency oscillation parameter identification. These methods generally outperform Prony analysis in parameter estimation. Nevertheless, both Prony and SSI techniques face challenges in accurately estimating model order under high-noise conditions, often leading to misidentification of oscillatory modes.

Despite the relative promise of these recent methods, their accuracy remains compromised in noisy signal environments. In response, this paper developed a spectral analysis approach based on PMU measurement data, utilizing Power Spectral Density (PSD) and Cross-Spectral Density (CSD) functions. This method aims to reduce noise sensitivity while enabling more accurate detection of low-frequency oscillations.

The remainder of this paper is organized as follows: Section 2 outlines the theoretical background of small-signal stability in power systems. Section 3 details the PSD and CSD methodologies. Section 4 introduces the IEEE 14-bus and 39-bus test systems and describes the simulation scenarios. Section 5 presents and discusses the simulation results. Finally, Section 6 offers conclusions and suggestions for future research.

II. Small-Signal Stability Fundamentals

In multi-machine power systems, small-signal stability is commonly defined as follows [2]:

"Small-signal stability refers to the ability of a power system to return to a steady operating condition following a small physical disturbance."

A fundamental assumption in this definition is that the system maintains coherence and that the oscillations remain limited in magnitude following a disturbance. Consequently, this form of stability is commonly known as small-signal stability.

A. Rotor Angle Stability

When a disturbance takes place in the system, the rotors of synchronous generators experience acceleration, resulting in variations in rotor angle and speed. In extreme cases, these deviations may lead to a loss of synchronism among generators. This behavior is typically represented by the swing equation. To facilitate stability analysis in multi-machine systems, the classical Single-Machine Infinite Bus (SMIB) model is often employed as a simplification. Figure

1 illustrates the simplified representation of an SMIB system.

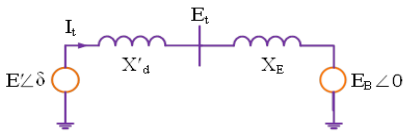

Fig. 1. Simplified SMIB System Model [5]

For an n-machine system, the motion equation of the i[th] machine is given by:

$$\frac{d\omega_i}{dt} = \frac{\omega_i}{2H_i}(P_{mech_i} - P_{e_i} - P_{D_i}) \quad (1)$$

Here, H_i is the inertia constant, ω_i is the rotor speed, P_{mech_i} and P_{e_i} are the mechanical and electrical powers, and P_{D_i} represents the damping power (a non-physical term used to model system damping).

According to Figure 1, the system current and apparent power can be defined as:

$$I_t = \frac{E'\angle\delta - E_B\angle 0}{jX_T} \;.\; X_T = X'_d + X_E \quad (2)$$

$$S' = P + jQ' = E'I_t^* = \frac{E'E_B \sin\delta}{X_T} + j\frac{E'(E' - E_B\cos\delta)}{X_T} \quad (3)$$

where:

E_B: Infinite bus voltage

E': Internal transient voltage

X_T: Total reactance (machine + line)

δ: Rotor angle (the angular difference between E' and E_B)

In the per-unit system and under small deviation assumptions, the electrical torque equals the electrical power. Hence:

$$P_e(\delta) = T_e(\delta) = \frac{E'E_B \sin\delta}{X_T} \quad (4)$$

As illustrated in Figure 2, rotor angle oscillations correspond directly to variations in power. This relationship forms the basis for measurement-based techniques used to evaluate small-signal stability.

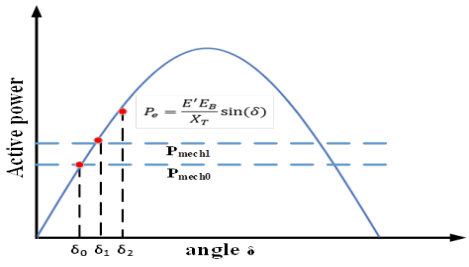

Fig. 2. Rotor Angle vs. Power Curve

Electromechanical oscillations naturally exist in power systems and depend on the slope of the $P-\delta$ curve. A steeper slope corresponds to a smaller $\Delta\delta$ for the same ΔP, implying a higher oscillation frequency [5].

From equation (4), the derivative of the electrical torque with respect to δ is:

$$\Delta T_e(\delta) = \frac{\partial T_e}{\partial\delta}\Delta\delta\frac{E'E_B\cos\delta_0}{X_T}\Delta\delta = K_S\Delta\delta \quad (5)$$

Here, K_S is the synchronizing coefficient. The linearized swing equation can be expressed as:

$$\frac{d}{dt}\Delta\omega_r = \frac{1}{2H}(T_m - T_e - K_D\Delta\omega_r) \quad (6)$$

$$\frac{d}{dt}\Delta\delta = \omega_0\Delta\omega_r \quad (7)$$

where:

$\Delta\omega_r$: Rotor speed deviation

δ: Rotor angle

ω_0: Base electrical speed

K_D: Damping coefficient

In state-space form:

$$\frac{d}{dt}\begin{bmatrix}\Delta\omega_r\\ \Delta\delta\end{bmatrix} = \begin{bmatrix}\frac{-K_D}{2H} & \frac{-K_S}{2H}\\ \omega_0 & 0\end{bmatrix}\begin{bmatrix}\Delta\omega_r\\ \Delta\delta\end{bmatrix} + \begin{bmatrix}\frac{1}{2H}\\ 0\end{bmatrix}\Delta T_m \quad (8)$$

Or more compactly:

$$\Delta\dot{X} = A\Delta X + BU \quad (9)$$

Here, A is the system state matrix. The eigenvalues of A determine system stability and form the foundation of model-based techniques such as modal analysis. Obtaining this matrix, however, requires precise knowledge of network dynamic parameters and accurate modeling of all dynamic elements.

III. Developed method

In future power systems, the use of signal processing techniques will become indispensable. The introduction of Phasor Measurement Units (PMUs) and the advancement of Wide-Area Monitoring Systems (WAMS) have made high-resolution, time-synchronized measurement data readily available to control centers. Within this framework, and assuming full system observability, spectral analysis methods such as Power Spectral Density (PSD) and Cross-Spectral Density (CSD) are developed as effective tools for assessing small-signal stability using PMU data.

B. Mathematical Frameworks

Assuming small disturbances in a multi-machine power system, the linearized differential equations around a stable operating point can be expressed as follows [2–5]:

$$\dot{\underline{x}}(t) = A\underline{x}(t) + B\underline{u}(t) \quad (10)$$

In typical multi-machine power systems, the input vector $\underline{u}(t)$ is modeled as a random disturbance caused by stochastic load switching events. Using eigenvalue decomposition, the system equations in (10) can be diagonalized. The eigenvalues and corresponding eigenvectors are defined as:

$$|\lambda_i I - A| = 0 \quad (11)$$

$$AR_i = \lambda_i R_i \quad (12)$$

$$L_i A = \lambda_i L_i \quad (13)$$

where λ_i is the i-th eigenvalue, and R_i and L_i are the corresponding right and left eigenvectors, respectively. The identity matrix I is of size $n \times n$. These eigenvectors can be organized into matrices:

$$R = [R_1 \dots R_n] \quad (14)$$

$$L = \begin{bmatrix} L_1 \\ \vdots \\ L_n \end{bmatrix}$$

These matrices satisfy the biorthogonality condition:

$$R \times L = I \tag{15}$$

A linear transformation is applied as:

$$z_i(t) = l_i\, x(t) \tag{16}$$

This leads to the diagonalized system:

$$L \times A \times R = \mathrm{diag}(\lambda_i) \tag{17}$$

Thus, the system dynamics are transformed into modal coordinates:

$$\dot{z}_i(t) = \lambda_i z_i(t) + l_i B u(t) \tag{18}$$

Here, $z_i(t)$ represents the response of the i-th mode to the input $u(t)$. Each state can then be reconstructed using the right eigenvectors:

$$x(t) = \sum_{i=1}^{n} z_i(t) r_i \tag{19}$$

To analyze modal contributions in the frequency domain, we define the spectral functions [31]:

$$S_{kl}(\omega) = \lim_{T\to\infty} \frac{1}{T} E\{Y_k^*(\omega) Y_l(\omega)\} \tag{20}$$

$$S_{kk}(\omega) = \lim_{T\to\infty} \frac{1}{T} E\{Y_k^*(\omega) Y_k(\omega)\} \tag{21}$$

Here, $S_{kl}(\omega)$ is the cross-spectral density (CSD) between two signals y_k and y_l, and $S_{kk}(\omega)$ is the power spectral density (PSD) of signal y_k. The terms $Y_k(\omega)$and $Y_l(\omega)$ are Fourier transforms of the respective time-domain signals, and $E\{\bullet\}$ is the expectation operator.

$$S_{kl}(\omega) = \lim_{T\to\infty} \frac{1}{T} E\{(\sum_{r=1}^{n} Z_r(\omega) R_{r,k})^* (\sum_{p=1}^{n} Z_p(\omega) R_{p,l})\} \tag{22}$$

By applying the Fourier transform to equation (18):

$$Z_i(\omega) = \frac{L_i B U(\omega)}{j\omega - \lambda_i} \tag{23}$$

Assuming λ_i is a lightly damped mode

$$\lambda_i = \alpha_i + j\omega_i \tag{24}$$

where $\alpha_i \ll \omega_i$, and substituting $\omega = \omega_i$ into the spectral expression, we approximate:

$$S_{kl}(\omega_i) \cong \lim_{T\to\infty} \frac{1}{T} E\{(Z_i(\omega_i) R_{i.k})^* (Z_i(\omega_i) R_{i.l})\} \tag{25}$$

Since $R_{i.k}$ and $R_{i.l}$ are constants:

$$S_{kl}(\omega_i) \cong R_{i.k}{}^* R_{i.l} \left[\lim_{T\to\infty} \frac{1}{T} E\{|Z_i(\omega_i)|^2\}\right] \tag{26}$$

Due to the stochastic nature of disturbances, this expectation term converges to a fundamental constant representing the variance at the mode frequency. Thus, the CSD angle can be approximated as:

$$\angle S_{kl}(\omega_i) \cong \angle R_{i.l} - \angle R_{i.k} \tag{27}$$

If $k = 1$, the PSD of the signal becomes:

$$S_{kk}(\omega_i) \cong |R_{i.k}|^2 \left[\lim_{T\to\infty} \frac{1}{T} E\{|Z_i(\omega_i)|^2\}\right] \tag{28}$$

Equations (27) and (28) are used to estimate the oscillation mode shape. Accurate PSD and CSD estimation requires synchronized measurements over a sufficiently long time interval. In this paper, Welch's method is employed for estimating the PSD and CSD from PMU data.

Using Welch averaging:

$$S_x^W(\omega_k) \triangleq \frac{1}{K} \sum_{m=0}^{K-1} P_{x_{m.M}}(\omega_k) \tag{29}$$

For a rectangular window ω_n, the periodograms are computed from non-overlapping data blocks. With other windows, overlapping frames are typically used.

IV. Case Study

To assess the effectiveness of the proposed PSD and CSD methods in estimating local and inter-area oscillatory modes within multi-machine power systems, simulations are performed on two standard IEEE test systems—the 14-bus and 39-bus networks. The simulations consider both ideal (noise-free) and noisy measurement conditions. Furthermore, the results are compared against those obtained from modal analysis, a model-based approach, as well as Prony analysis, a measurement-based (model-free) technique.

Dynamic simulations and modal analysis are performed using DIgSILENT PowerFactory 15.1, which includes predefined 14-bus and 39-bus standard systems. In order to implement the Prony method, the Signal Processing Toolbox in MATLAB R2022a is utilized.

C. 14-Bus and 39-Bus Description

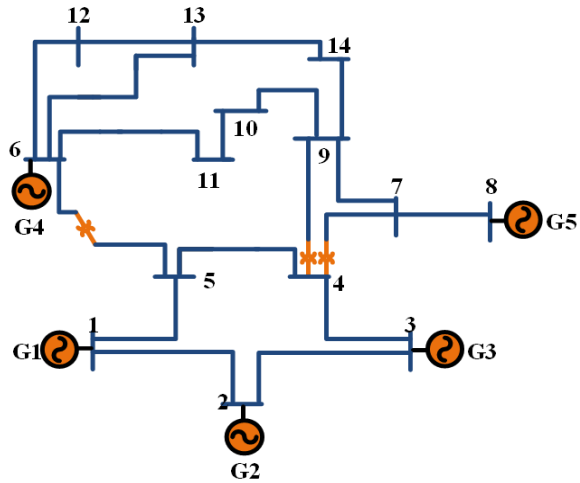

Fig. 3. IEEE 14-Bus Single-Line Diagram

The IEEE 14-bus system includes:

- 14 buses
- 5 generator units
- 11 loads
- 20 transmission lines
- 3 transformers connecting different voltage levels

Nominal voltage levels:

- Buses 1 to 5: 132 kV

- Buses 6, 9 to 14: 33 kV
- Bus 7: 1 kV
- Bus 8: 11 kV

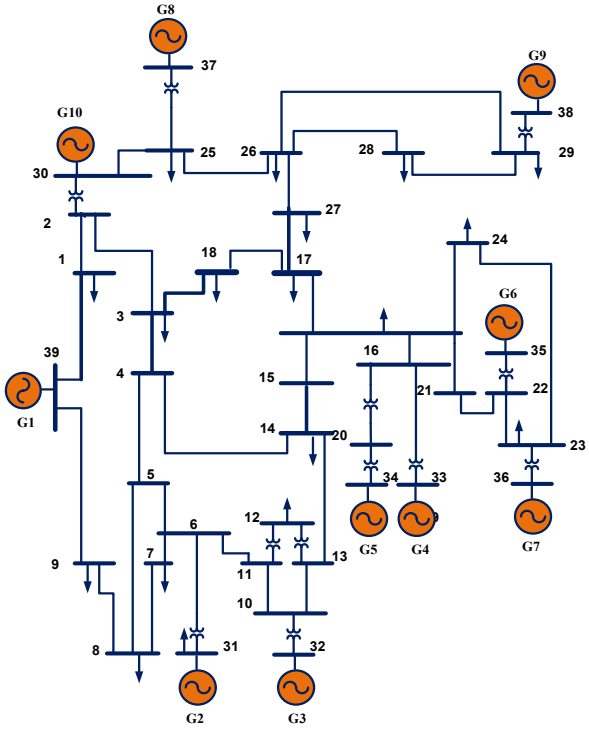

Fig. 4. IEEE 39-Bus Single-Line Diagram

All data are obtained from [32], representing a standard benchmark for power system stability analysis.

The IEEE 39-bus system is well known as a 10-machine New-England power system, where Generator 1 represents the aggregation of a large number of generators. The system includes [33]:

- 39 buses
- 10 generator units
- 18 loads
- 46 transmission lines
- 12 transformers connecting different voltage levels

D. Simulation Scenarios

To evaluate the proposed method, two simulation scenarios are considered for both the 14-bus and 39-bus test systems. In each system, after dynamic simulations, modal analysis, a developed method, and the Prony algorithm are implemented to compare their effectiveness.

- **Ideal Case**:

In this scenario, the measured signal is analyzed directly. For instance, variations of active power flow or bus frequency are recorded immediately following a small-signal disturbance. These measurements are captured directly from signal recordings in DIgSILENT and are used as inputs for comparison of different approaches.

- **Noisy Case**:

To emulate the uncertainties present in actual measurement conditions, Gaussian white noise is added to the recorded signals. This simulates real-world PMU data that may be affected by noise. After the disturbance, a white Gaussian noise with zero mean is added to the measured signals, which are then used as inputs for comparison of different approaches.

E. Modal Analysis

Before applying measurement-based methods, oscillatory modes of 14-bus and 39-bus systems are calculated using modal eigenvalue analysis to serve as the basis for comparisons. It should be noted that modal analysis is done using predefined models of DIgSILENT Power Factory, where the eigenvalues are calculated using the QR method through system reduction. The obtained eigenvalue plots, indicating oscillatory modes of 14-bus and 39-bus systems, are shown in Figure 5 and Figure 6, respectively.

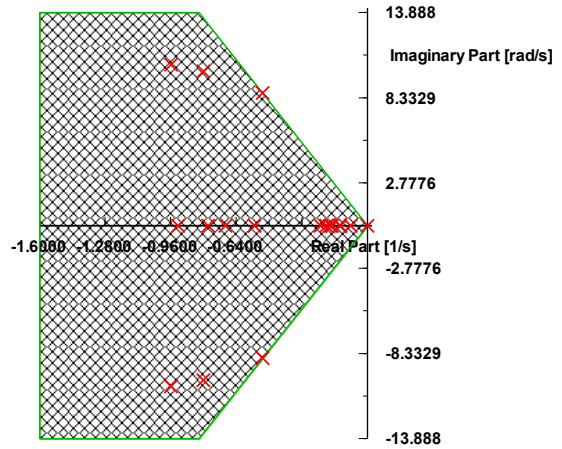

Fig. 5. Eigenvalue plot of 14-bus system

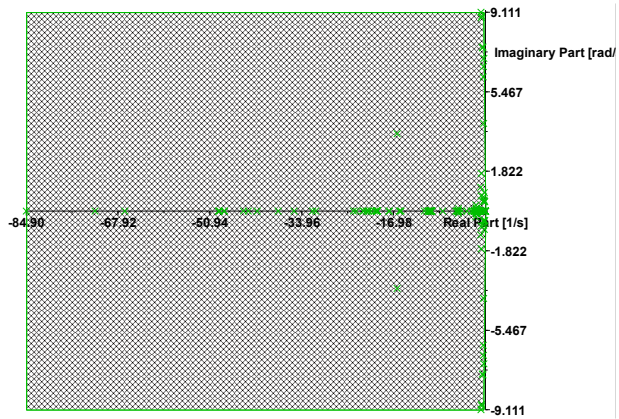

Fig. 6. Eigenvalue plot of 39-bus system

As observed in Figure 5 and Figure 6, there are four dominant oscillatory modes in the 14-bus and nine oscillatory modes in the 39-bus systems, whose specifications are listed in the following tables, respectively.

TABLE I OSCILLATORY MODES OF THE 14-BUS SYSTEM

Mode No.	Frequency (Hz)	Damping (1/s)	Mode Shape
1	1.36	0.51	G_1, G_2 vs. G_5
2	1.60	0.80	G_1 vs. G_3
3	1.66	0.96	G_3 vs. G_2
4	2.21	1.56	G_1 vs. G_2

TABLE II OSCILLATORY MODES OF THE 39-BUS SYSTEM

Mode No.	Frequency (Hz)	Damping (1/s)	Mode Shape
1	1.32	1.51	G_8 vs. G_{10}
2	1.13	1.08	G_9 vs. G_8, G_{10}
3	1.30	0.99	G_5 vs. G_4, G_6, G_7
4	1.30	1.01	G_5 vs. G_4, G_6
5	1.07	0.85	G_5, G_4 vs. G_7, G_6
6	1.08	0.61	G_3 vs. G_2
7	0.87	0.54	G_9 vs. G_2, G_3
8	0.94	0.52	G_4-G_7 vs. G_2, G_3
9	0.66	0.37	G_1 vs. grid

F. Developed Method Simulations

To evaluate the effectiveness of the developed methods, simulations are carried out under two scenarios: Ideal and Noisy conditions, and the obtained results are compared with those from modal analysis.

Ideal Case Simulation:

In this case, simulations are conducted on both 14-bus and 39-bus systems. In each system, the oscillatory modes are identified using a developed method and the Prony algorithm as measurement-based methods. In addition, the results are verified compared to a realistic modal specification that has been obtained via modal analysis as a model-based method.

IEEE 14-bus test system

In the 14-bus system, a three-phase-to-ground fault is simulated on the transmission line, connecting bus2-bus4, at second 2 for a duration of 200ms. The fault is cleared at 2.2 s, occurring at the midpoint of the 132 kV transmission line. In practice, synchronized rotor angle and rotor speed signals are not directly measurable, although they contain detailed modal information. Thus, the evaluation is performed using PMU-accessible signals such as active power.

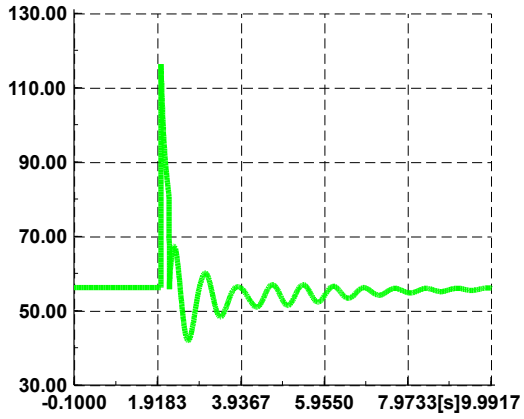

Fig. 7. Active power variation on Line$_{2-4}$ under 200-ms fault in 14-bus system

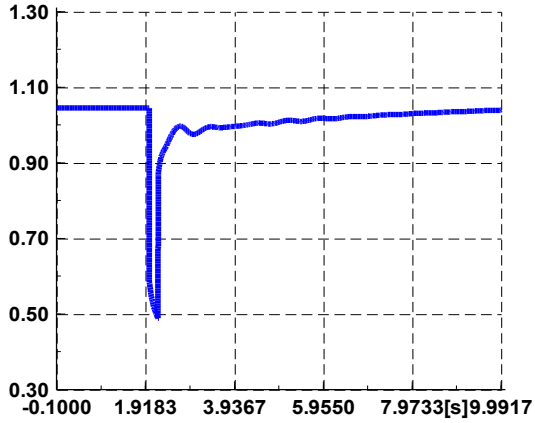

Fig. 8. Voltage variation at Bus 2 under 200-ms fault in 14-bus system

Since PMUs can capture time-synchronized power and voltage data, these are used in the analysis. As shown in Figure 7, the power flow initially measures 56.17 MW, and after the disturbance, the system stabilizes, and the power flow returns to its original level. Similarly, the per-unit voltage at Bus 2, shown in Figure 8, also returns to pre-fault levels. The PSD method is then applied to the active power signal of Line$_{2-4}$. From Figure 9, two dominant oscillation frequencies—1.66 Hz and 1.36 Hz—are identified, corresponding to Modes 1 and 3 in Table 1. This confirms that the PSD method can accurately estimate modal frequencies without requiring the system model. From repeated simulations, the following key insights were obtained:

- Oscillatory modes are more evident in line power flow signals than in bus voltage signals.
- Other oscillatory modes can also be identified in different line power signals. For better reliability, it is recommended to use multiple signals for robust mode estimation.
- The time window for PSD input must start a few milliseconds after fault clearance (e.g., ~100 ms) and end before the oscillations have fully decayed.

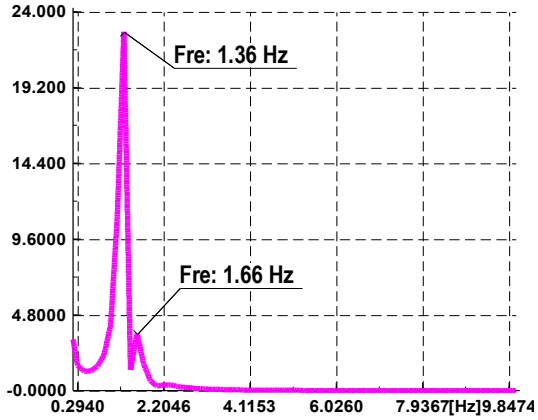

Fig. 9. PSD result for Line$_{2-4}$ power signal in 14-bus system

To compute the CSD, the voltage angle of one generator bus must be used as a reference. In the IEEE 14-bus system, Generator 1 (with 1.06pu and 0° angle) is chosen as the reference. Then, CSD is applied to the generator's bus frequency signals. The variation of generator buses' frequency during the fault occurrence and after its clearance is shown in Figure 10.

Corresponding CSD to Figure 10 is illustrated in Figure 11. As can be seen in Figure 11, at 1.36 Hz, Buses 1, 2, and 3 oscillate against Buses 6 and 8. At 1.66 Hz, Buses 3 and 6 oscillate against Buses 1 and 8. These coherent groupings confirm the effectiveness of the CSD method in identifying mode shapes.

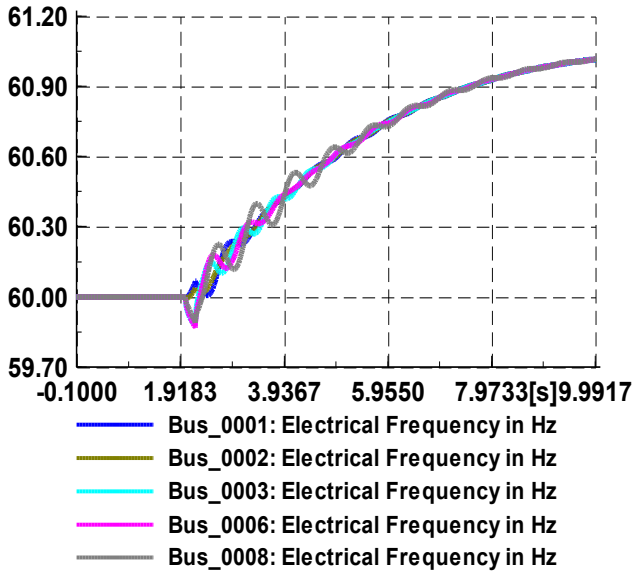

Fig. 10. Generator bus frequency variations during the 200-ms fault in 14-bus system

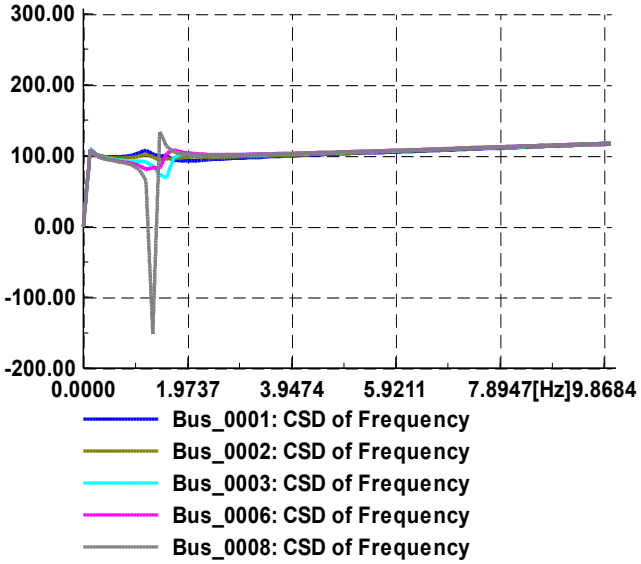

Fig. 11. CSD phase analysis of generator bus frequencies in 14-bus system

IEEE 39-bus test system

In the 14-bus system, a three-phase-to-ground fault is simulated on the transmission line, connecting bus14-bus4, at second 2 for a duration of 200^{ms}. The fault is cleared at 2.2 s, occurring at the midpoint of the transmission line. In practice, synchronized rotor angle and rotor speed signals are not directly measurable, although they contain detailed modal information. Thus, the evaluation is performed using PMU-accessible signals such as active power and bus voltage. The variation of the total active power of line 14-4 is indicated in Figure 12. Same as previous simulations, the PSD is applied to the active power signal captured from PMU data. The corresponding PSD to Figure 12 is illustrated in Figure 13.

As can be observed in Figure 13, the dominant oscillation frequency of 0.66 Hz is well identified, corresponding to Mode 9 in Table II. This confirms that the PSD method can accurately estimate modal frequencies without requiring the system model. It should be noted that other modes could be obtained by applying PSD to different power signal variations. The power variation of Line14-4 provides the exact information of the ninth mode.

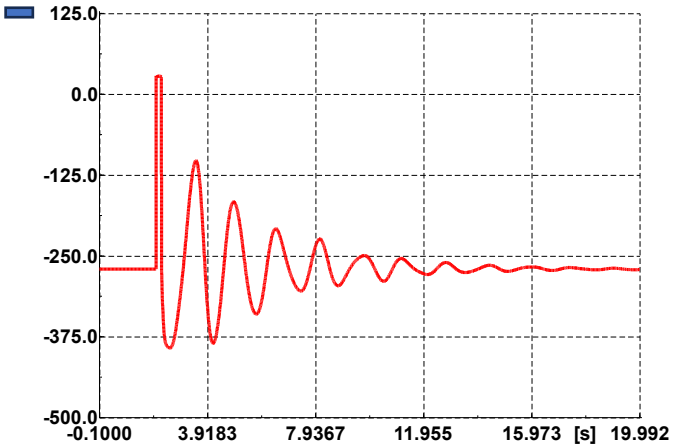

Fig. 12. Active power variation on Line$_{14\text{-}4}$ under 200-ms fault in 39-bus system

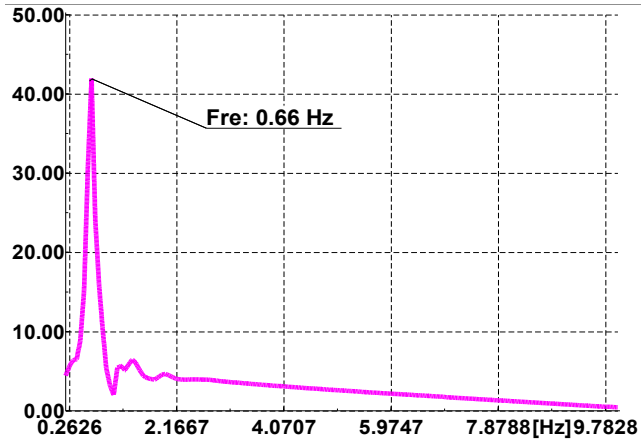

Fig. 13. PSD result for Line$_{14\text{-}4}$ power signal in 39-bus system

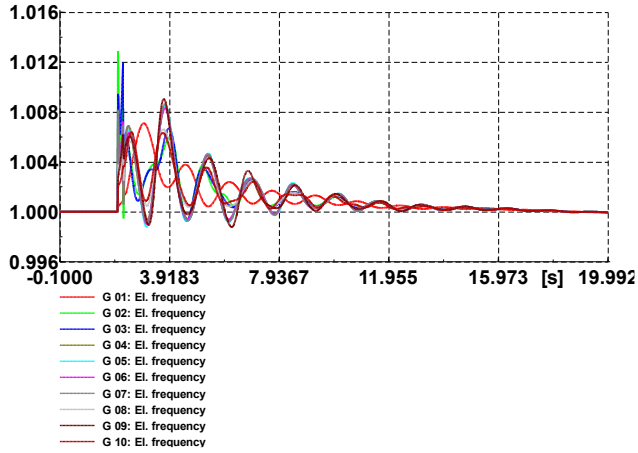

Fig. 14. Generator bus frequency variations during the 200-ms fault in 39-bus system

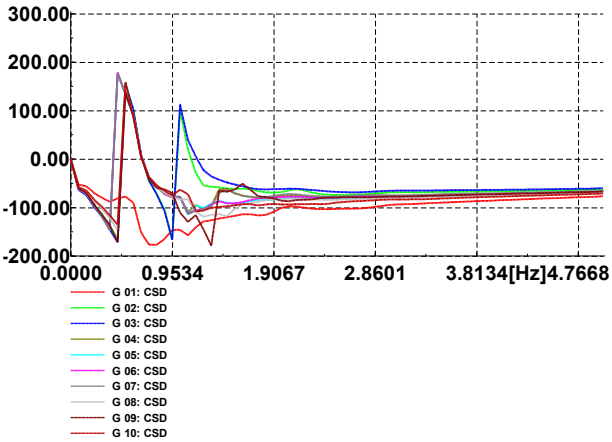

Fig. 15. CSD phase analysis of generator bus frequencies in 39-bus system

To calculate the Cross-Spectral Density (CSD), the voltage angle of a generator bus must be considered as a reference. In the 39-bus system, Generator 1—which represents an aggregation of multiple generators—is selected as this reference. The frequency variations of all ten generator buses following the three-phase fault are depicted in Figure 14. Subsequently, CSD is applied to the frequency signals of the generator buses, with the results shown in Figure 15. As illustrated, at approximately 0.66 Hz, Generator 1 (red line) oscillates against the other generators. Figure 15 provides additional detailed information regarding the oscillatory interactions among generators across the grid, which correspond directly to the mode shapes of various oscillatory modes. While multiple details can be extracted, the primary focus here is the generator's behavior at the 0.66 Hz frequency. These coherent groupings validate the effectiveness of the CSD method in accurately identifying mode shapes.

G. Simulation under Noisy Conditions (SNR = 30)

In this section, all simulations are repeated under the noisy conditions.

IEEE 14-bus test system

In this scenario, white Gaussian noise with an SNR of 30 is added to the active power flow signal of $Line_{2-4}$ in the 14-bus system. The results of the PSD analysis are presented in Figure 16. As shown, the two dominant frequencies—1.66 Hz and 1.36 Hz—are still clearly identifiable, while the peak magnitudes are a little bit lower in comparison to ideal conditions. After identifying the modal frequencies, the CSD function is applied to the noisy generator bus frequency signals (Figure 17).

The results indicate that the oscillatory behavior of the generators remains consistent with the ideal case. Despite the added noise, the CSD outputs are not significantly degraded, confirming the noise immunity of the proposed methods.

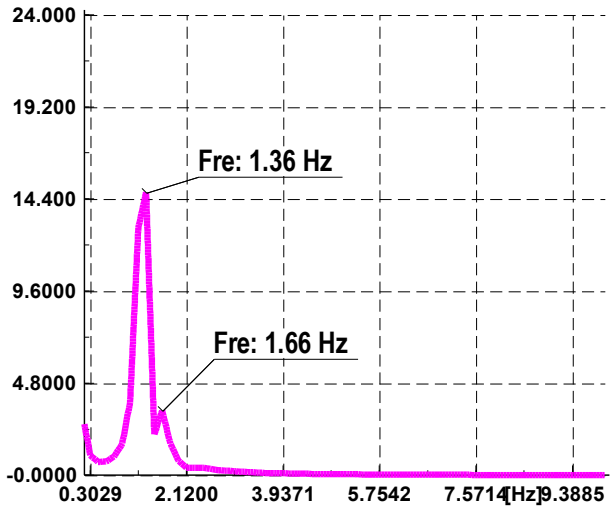

Fig. 16. PSD result for $Line_{2-4}$ with SNR = 30 in 14-bus system

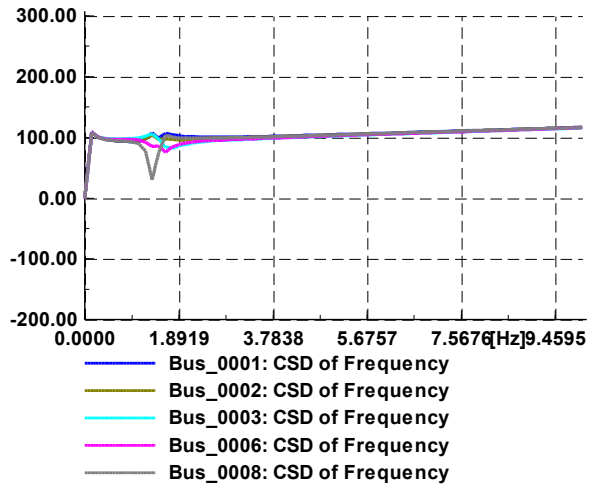

Fig. 17. Corresponding CSD to generator frequencies with SNR = 30 in 14-bus system

IEEE 39-bus test system

All the simulations are repeated for the 39-bus system under noisy conditions. The PSD corresponding to the active power flow signal of Line14-4 in the 39-bus system is indicated in Figure 18. As can be seen, the dominant frequency 0.66 Hz is still clearly identifiable, while the peak

magnitudes are a little bit lower in comparison to ideal conditions. After identifying the modal frequencies, the CSD function is applied to the noisy generator bus frequency signals. Corresponding CSD results are shown in Figure 19.

As can be seen, the oscillatory behavior of the generators remains consistent with the ideal case. Despite the added noise, the CSD outputs are not significantly degraded, confirming the noise immunity of the developed methods.

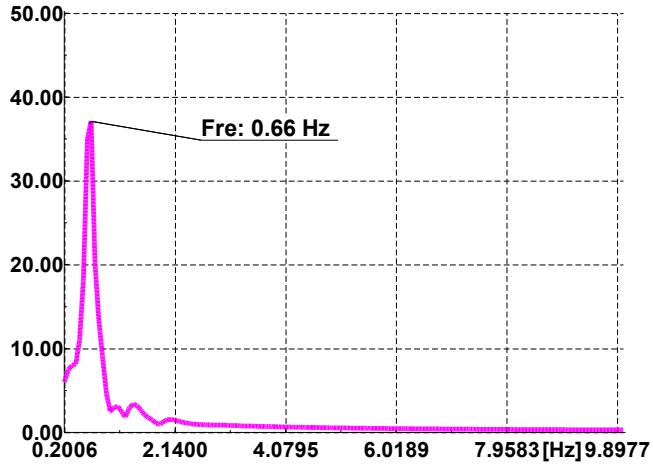

Fig. 18. PSD result for Line$_{14-4}$ with SNR = 30 in 39-bus system

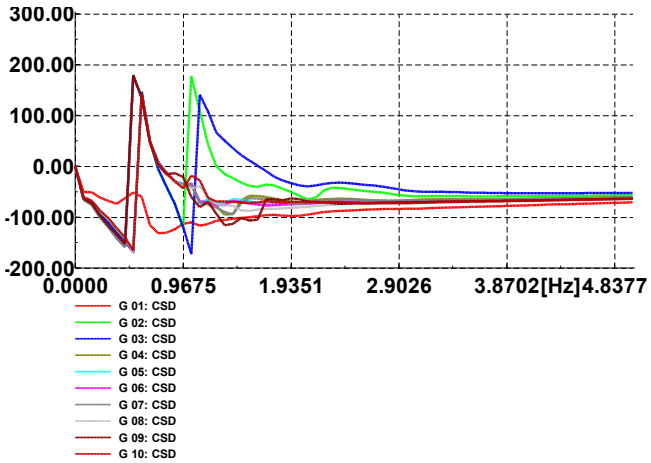

Fig. 19. Corresponding CSD to generator frequencies with SNR = 30 in 39-bus system

H. Prony Algorithm

In order to prove the robustness of the developed method, the results are compared with the Prony algorithm as a measurement-based method under ideal and noisy conditions. The comparison is done for the 39-bus case study. The same input data that has been used for PSD calculation is set as the Prony algorithm input.

It should be noted that the raw data obtained from the dynamic simulation is exported from DIgSILENT Power Factory version 15.1.7 and then imported to MATLAB R2022a, where the Prony algorithm is applied via Signal Processing Toolbox. Simulation results for the ideal case and

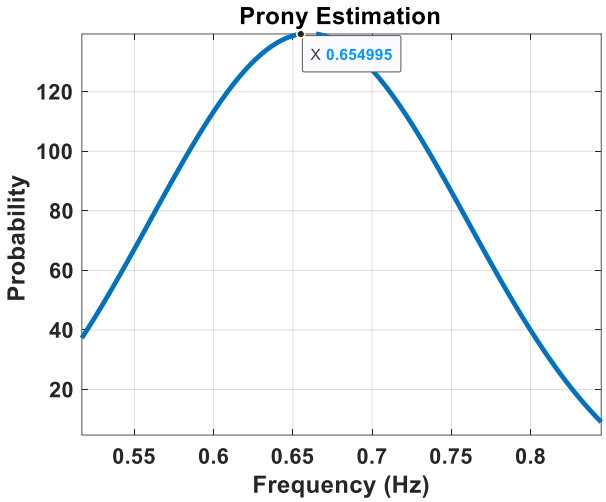

Fig. 20. Prony algorithm in ideal case in 39-bus system

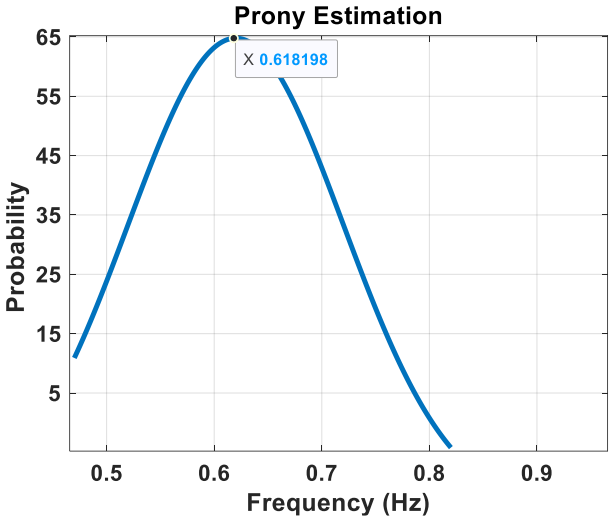

Fig. 21. Prony algorithm in noisy case in 39-bus system

It should be noted that the raw data obtained from the dynamic simulation is exported from DIgSILENT Power Factory version 15.1.7 and then imported to MATLAB R2022a, where the Prony algorithm is applied via Signal Processing Toolbox. Simulation results for the ideal case and noisy case are shown in Figure 20 and Figure 21, respectively.

As can be seen, in the ideal condition without considering noise, the Prony algorithm estimates the frequency near its real value, 0.66 Hz, with the minimum error. However, the probability plot in Figure 21 proves the Prony inefficiency under noisy conditions exactly as other papers in the literature review. Therefore, the Prony algorithm accuracy is highly degraded under noisy conditions.

I. Interpretation of Results

The comparative evaluation of model-based (modal analysis) and measurement-based (developed method and Prony algorithm) methods yields the following key findings:

- Model-based techniques, such as modal analysis, require accurate dynamic modeling of all system components, particularly synchronous generators. While this is feasible for small benchmark systems, such as the IEEE 14-bus, it becomes impractical for large interconnected power networks due to the lack of complete and precise dynamic data.
- A significant outcome of this study is that measurement-based methods can reveal oscillatory modes in various system signals. For PSD, long transmission line power signals are most suitable, while for CSD, bus frequencies are the best input signals.
- The timing of the analysis window is critical for measurement-based methods. The time window should begin a few milliseconds (approximately 100ms) after fault clearance and end before the oscillations fully decay. Early signal portions only reflect transient dynamics and do not accurately contain modal information.
- The estimated frequencies from the developed method closely match the results from modal analysis. For instance, modal analysis detects modes at 1.36 Hz and 1.60 Hz, while the developed method estimates them as 1.359 Hz and 1.659 Hz. Even under noisy conditions (SNR = 30), estimated values remain highly accurate.
- Whether in ideal or noisy environments, the CSD method correctly identifies oscillatory relationships among generators. Given its speed and accuracy, it can be used for preventive control and mitigation of wide-area blackouts.
- An important operational insight is that long inter-area transmission lines are particularly prone to initiating system-wide instability, especially when heavily loaded. Monitoring power flow across these lines can help detect early signs of oscillations and prevent system collapse.
- Comparison between the developed method and the Prony algorithm, as a measurement-based method, shows that the Prony algorithm accuracy is highly prone to noisy data. However, in the ideal condition, the Prony algorithm estimates the frequency very accurately.

V. Conclusion and Future Work

According to the literature, power oscillations—particularly under high loading conditions—can lead to the loss of synchronism in power systems. Therefore, accurately detecting and responding to these oscillations in real time is critical for ensuring the stability of modern multi-machine power systems and preventing blackouts. Model-based methods are often unsuitable for large-scale networks due to their reliance on complete and accurate dynamic models. With the emergence of PMUs, measurement-based approaches have become essential. While several measurement-based methods have been proposed, many suffer from noise sensitivity or computational inefficiency.

In this paper, PSD and CSD techniques are developed as efficient tools for small-signal stability assessment using only synchronized PMU data. In addition, the Prony algorithm accuracy degradation as a measurement-based method under noisy data has been proven.

Simulation results on the IEEE 14-bus and 39-bus systems demonstrate that the developed method can accurately estimate oscillatory modes—even in the presence of measurement noise—without requiring knowledge of system model order or the entire network. The results are also validated against modal eigenvalue analysis from DIgSILENT, confirming their high accuracy.

J. Recommendations for Future Work:

- The developed methods should be applied to larger benchmark systems, such as the IEEE 118-bus system, to thoroughly evaluate their scalability and overall performance.
- This study focused exclusively on white Gaussian noise; however, real-world systems often experience colored noise, which incorporates system dynamics and can affect accuracy. Future research should investigate the effects of different noise types on results.
- The selection of signals plays a critical role in the accuracy of measurement-based approaches. Even the most advanced identification techniques may fail if the input signals do not contain pertinent dynamic information. Therefore, it is vital to choose signals that capture steady-state modal behavior rather than transient responses.

REFERENCES

[1] Phadke, Arun G. "Synchronized phasor measurements-a historical overview." In IEEE/PES transmission and distribution conference and exhibition, vol. 1, pp. 476–479. IEEE, 2002.

[2] Kundur, Prabha. "Power system stability." Power system stability and control 10 (2007): 7–1.

[3] Maleki Rizi, Masoud, Saeed Abazari, and Nima Mahdian. "Dynamic Stability Improvement of Power System with Simultaneous and Coordinated Control of DFIG and UPFC using LMI." International Journal of Industrial Electronics Control and Optimization 4, no. 3 (2021): 341-353.

[4] Kundur, Prabha, John Paserba, Venkat Ajjarapu, Göran Andersson, Anjan Bose, Claudio Canizares, Nikos Hatziargyriou et al. "Definition and classification of power system stability IEEE/CIGRE joint task force on stability terms and definitions." Power Systems, IEEE Transactions on 19, no. 3 (2004): 1387-1401

[5] Farmer, Richard G. "Power system dynamics and stability." The Electric Power Engineering Handbook Series, CRC Press LLC, 2001.

[6] Babaali, AmirHossein, and Mohammad Taghi Ameli. "Multi-class short-term voltage stability assessment considering the missing data."

International Journal of Industrial Electronics Control and Optimization (2025).

[7] IEEE Working Group. "IEEE Guide for Identification, Testing and Evaluation of the Dynamic Performance of Excitation Control Systems." 421–2.

[8] Pourbeik, Pouyan, Prabha S. Kundur, and Carson W. Taylor. "The anatomy of a power grid blackout-root: causes and dynamics of recent major blackouts." IEEE Power and Energy Magazine 4, no. 5 (2006): 22–29.

[9] Han, Lei, Yibing Wang, Yu Zhang, Cheng Lu, Chengwei Fei, and Yongjun Zhao. "Competitive cracking behavior and microscopic mechanism of Ni-based superalloy blade respecting accelerated CCF failure." International Journal of Fatigue 150 (2021): 106306.

[10] Yu, Yiping, Yaling Shen, Xiang Zhang, Jiyun Zhu, and Jiajia Du. "The load oscillation energy and its effect on low-frequency oscillation in power systems." In 2015, the 5th International Conference on Electric Utility Deregulation and Restructuring and Power Technologies (DRPT), pp. 1336–1341. IEEE, 2015.

[11] Jami, Mehran. "Virtual inertia control and small-signal stability analysis of electric vehicle." International Journal of Industrial Electronics Control and Optimization 6, no. 4 (2023): 261-270.

[12] Cai, Guowei, Deyou Yang, Ying Jiao, and Chunyu Shao. "Power system oscillation mode analysis and parameter determination of PSS based on stochastic subspace identification." In 2009 Asia-Pacific Power and Energy Engineering Conference, pp. 1–6. IEEE, 2009.

[13] Suzuki, Naoto, Takashi Hiyama, and Takahiko Funakoshi. "Real time FFT based on-line identification of power system oscillation modes." IEEJ Transactions on Power and Energy 120, no. 2 (2000): 134–140.

[14] Rueda, José L., Carlos A. Juárez, and István Erlich. "Wavelet-based analysis of power system low-frequency electromechanical oscillations." IEEE Transactions on Power Systems 26, no. 3 (2011): 1733–1743.

[15] Hauer, J. F. "Application of Prony analysis to the determination of modal content and equivalent models for measured power system response." IEEE Transactions on Power Systems 6, no. 3 (1991): 1062–1068.

[16] Teshnehlab, Mohamad, and Mehdi Aliyari-shoredeli. "Fault detection and identification of high dimension system by GLOLIMOT." International Journal of Industrial Electronics Control and Optimization 2, no. 4 (2019): 331-342.

[17] Wies, Richard W., John W. Pierre, and Daniel J. Trudnowski. "Use of ARMA block processing for estimating stationary low-frequency electromechanical modes of power systems." IEEE Transactions on Power Systems 18, no. 1 (2003): 167-173.

[18] M. A. Heydari , M. HassanniaKheibari and G. Sadeghi, "Control of a shunt Active Power Filter with Voltage Source Model to Improve the Power Quality Performance," International Journal of Industrial Electronics Control and Optimization, 7 3 (2024): 247-255, doi: 10.22111/ieco.2024.48277.1547.

[19] Poisson, Olivier, Pascal Rioual, and Michel Meunier. "Detection and measurement of power quality disturbances using wavelet transform." IEEE Transactions on Power Delivery 15, no. 3 (2000): 1039–1044.

[20] Trudnowski, Daniel J., J. M. Johnson, and John F. Hauer. "Making Prony analysis more accurate using multiple signals." IEEE Transactions on Power Systems 14, no. 1 (1999): 226-231.

[21] Qi, Li, Lewei Qian, Stephen Woodruff, and David Cartes. "Prony analysis for power system transient harmonics." EURASIP Journal on Applied Signal Processing 2007, no. 1 (2007): 170–170.

[22] Grund, C. E., J. J. Paserba, J. F. Hauer, and S. L. Nilsson. "Comparison of Prony and eigenanalysis for power system control design." Power Systems, IEEE Transactions on 8, no. 3 (1993): 964–971.

[23] Xiao, Jinyu, Xiaorong Xie, Yingduo Han, and Jingtao Wu. "Dynamic tracking of low-frequency oscillations with improved Prony method in wide-area measurement system." In the Power Engineering Society General Meeting, 2018. IEEE, pp. 1104-1109. IEEE.

[24] Tripathy, P., S. C. Srivastava, and S. N. Singh. "A noise space decomposition based method for identifying low frequency oscillations using synchro-phasor measurements." In the 2010 IEEE Power and Energy Society General Meeting, pp. 1–6. IEEE, 2010.

[25] Ye, Hua, Yutian Liu, and Xinsheng Niu. "Low frequency oscillation analysis and damping based on Prony method and sparse eigenvalue technique." In Networking, Sensing and Control, 2006. ICNSC'06. Proceedings of the 2006 IEEE International Conference on, pp. 1006–1010. IEEE, 2006.

[26] Tripath, P., S. C. Srivastava, and S. N. Singh. "An improved Prony method for identifying low frequency oscillations using synchro-phasor measurements." InPower Systems, 2009. ICPS'09. International Conference on, pp. 1–5. IEEE, 2009.

[27] Zhao, Yishu, Yang Gao, Zhijian Hu, Yongjun Yang, Jie Zhan, and Yan Zhang. "A new method of identifying the low frequency oscillations of power systems." In Energy and Environment Technology, 2009. ICEET'09. International Conference on, vol. 2, pp. 19-22. IEEE, 2009.

[28] Tripathy, P., S. C. Srivastava, and S. N. Singh. "A noise space decomposition based method for identifying low frequency oscillations using synchro-phasor measurements." In the 2010 IEEE Power and Energy Society General Meeting, pp. 1–6. IEEE, 2010.

[29] Fangzong, Wang, and Li Chengcheng. "Online Identification of Low-Frequency Oscillation Based on Principal Component Analysis Subspace Tracking Algorithm." In Power and Energy Engineering Conference (APPEEC), 2010 Asia-Pacific, pp. 1–4. IEEE, 2010.

[30] Yang, Jann N., Ying Lei, Shuwen Pan, and Norden Huang. "System identification of linear structures based on Hilbert–Huang spectral analysis. Part 1: normal modes." Earthquake engineering & structural dynamics 32, no. 9 (2003): 1443-1467.

[31] Osipov, Denis, Stavros Konstantinopoulos, and Joe H. Chow. "A cross-power spectral density method for locating oscillation sources using synchrophasor measurements." IEEE Transactions on Power Systems 2022.
[32] L. L. Freris, A. M. Sasson: “Investigation of the load-flow problem”, PROC. IEEE, Vol. 115, No. 10, October 1968, pp. 1459–1470.
[33] DIgSILENT GmbH, PowerFactory User Manual, Version 15.1, 2022. (Reference for the software tool containing the IEEE 39-bus system).

Zivar Rigi received her B.Sc degree in Electrical engineering from the Islamic Azad Zahedan Univercity,Iran in 2012. Now she is pursuing M.Sc degree in Power Electrical at the Islamic Azad Zahedan Univercity, Iran. Her research interests include power systems, distribution networks and demand response.

Mahdi Hassanniakheibari was born in Gonabad, Iran, in 1987. He received his PhD in Power Electrical Engineering from the Islamic Azad University, Science and Research Branch, Tehran, Iran, in 2020. He is an Assistant Professor at the Islamic Azad University, Zahedan Branch. His research interests include power systems, distribution networks, demand response, and power electronic converters.